Thermochimica Acta, 112 (1987) 231–243
Elsevier Science Publishers B.V., Amsterdam – Printed in The Netherlands

SYNTHESIS OF γ-Fe_2O_3 BY THERMAL DECOMPOSITION OF $FeC_4H_4O_4 \cdot 4H_2O$

A. VENKATARAMAN, V.A. MUKHEDKAR *, M.M. RAHMAN, A.K. NIKUMBH and A.J. MUKHEDKAR

Department of Chemistry, University of Poona, Pune 411 007 (India)

(Received 7 July 1986)

ABSTRACT

Ferrous succinate tetrahydrate ($FeC_4H_4O_4 \cdot 4H_2O$) is prepared and its thermal decomposition is studied by means of simultaneous thermal analysis (TGA, DTA, DTG) curves supplemented with two probe d.c. electricial conductivity measurements under the atmospheres of static air, dynamic nitrogen and dynamic air. Dynamic air containing water vapour, was found to be the most suitable atmosphere for the synthesis of γ-Fe_2O_3. The isothermal decomposition study of $FeC_4H_4O_4 \cdot 4H_2O$ for various intermediate phases occurring at different ranges of temperature under the above atmospheres have been studied using infrared spectral studies, C and H analysis and X-ray diffraction data. This study revealed the formation of anhydrous carboxylate ($FeC_4H_4O_4$) which then oxidatively decomposes to α-Fe_2O_3 with the probable intermediates of FeO and Fe_3O_4 along with some $FeC_4H_4O_4$ and γ-Fe_2O_3. Both polar and non-polar gases were obtained during the decomposition of $FeC_4H_4O_4 \cdot 4H_2O$ under nitrogen atmosphere which were analysed using gas–liquid chromatography. The γ-Fe_2O_3 synthesised was studied for its magnetic and Mossbauer parameters. The scanning electron micrographs obtained showed γ-Fe_2O_3 particles to be spherical in shape.

INTRODUCTION

Gamma ferric oxide (γ-Fe_2O_3) is a very important magnetic tape recording material [1,2] which is widely used because of its ideal combination of such parameters as saturation magnetisation (M_S), coercive force (H_C) and squareness ratio (M_R/M_S) [3]. Generally, γ-Fe_2O_3 is used in the form of single-domain (SD) particles with acicular shape for a good signal to noise ratio on recording [3].

γ-Fe_2O_3 is obtained commercially from synthetic Goethite (α-FeO(OH)) involving stringent experimental conditions. Recently, the synthesis of γ-Fe_2O_3 by the thermal decomposition of ferrous oxalate has been reported [4,5]. The use of d.c. electrical conductivity measurement for synthesising

* Author to whom correspondence should be addressed.

0040-6031/87/$03.50

γ-Fe_2O_3 by thermal decomposition of ferrous oxalate dihydrate has been reported [6]. Other than ferrous oxalate dihydrate no other ferrous carboxylate has been found for the synthesis of γ-Fe_2O_3. This paper deals with a modified way of synthesising γ-Fe_2O_3 and studying its magnetic and Mossbauer parameters using ferrous succinate tetrahydrate ($FeC_4H_4O_4 \cdot 4H_2O$) as the starting material. Literature on the thermal decomposition of metal succinates is scarce [7–9]. Apart from the use of conventional thermal analysis techniques (TGA, DTA, DTG), the advantages of using a complementary technique (i.e., the use of d.c. electrical conductivity measurements under different atmospheres) during the thermal dehydration and decomposition of $FeC_4H_4O_4 \cdot 4H_2O$ is well envisaged.

EXPERIMENTAL

Apart from conventional solution chemistry precipitation techniques, various instrumental methods such as infrared spectrometry (IR), C and H analysis, X-ray powder diffraction (XRD), thermal analysis (TGA, DTA and DTG), two-probe d.c. electrical conductivity, scanning electron microscopy (SEM), high-field magnetic hysteresis loop tracer (HLT), initial magnetisation, Mossbauer spectroscopy and gas–liquid chromatography (GLC) are used.

The thermal analysis curves were recorded on a NERTZ instrument under static air, dynamic dry nitrogen and dynamic air atmospheres. The flow rate of nitrogen and dynamic air was 100 ml min^{-1} and the heating rate was 5°C min^{-1} for the static air atmosphere and 10°C min^{-1} for the dynamic air and dynamic dry nitrogen atmospheres. The d.c. electrical conductivity was measured on a Philips d.c. Micro Voltmeter PP 9004 instrument under static air, dynamic dry nitrogen, dynamic air and dynamic air containing water vapour [6]. The heating rate was adjusted to 10°C min^{-1} and the flow rate was maintained at 100 ml min^{-1}. The evolution of various gases during the thermal decomposition of $FeC_4H_4O_4 \cdot 4H_2O$ was recorded on Shimadzu RIA and Hewlett Packard instruments using nitrogen as the carrier gas.

The morphology of the γ-Fe_2O_3 particles was taken on a Cambridge Steroscan 150 instrument. The XRD of samples were carried out in a Philips X-ray diffractometer (PW 1730) using MoK_α radiation. The magnetic properties were measured on a high-field hysteresis loop tracer (HLT) and initial magnetisation unit. Mossbauer spectra were recorded on a constant acceleration Mossbauer spectrometer assembled in the University Department of Physics.

Preparation of $FeC_4H_4O_4 \cdot 4H_2O$

$FeC_4H_4O_4 \cdot 4H_2O$ was prepared by dissolving the metal carbonate in a solution of succinic acid under a dynamic (pure and dry) nitrogen atmo-

sphere [10]. The values of C and H analysis agreed with the calculated values within $\pm 0.4\%$. The IR spectrum showed frequencies corresponding to carboxylate group, hydroxyl group, metal oxygen, etc., and the bidentate linkage of the carboxylate group with the metal was observed on the basis of the difference between the anti-symmetric stretching and symmetric stretching frequencies. The XRD pattern showed the sample to be polycrystalline in nature and having low symmetry. The four molecules of water of crystallisation were confirmed on the basis of thermal analysis curves and d.c. electrical conductivity measurements.

RESULTS AND DISCUSSION

Static air atmosphere

The dehydration step of $FeC_4H_4O_4 \cdot 4H_2O$ in Fig. 1(a) could be detected by the presence of a strong endothermic peak at 94°C and also by a strong peak at the same temperature on the DTG curve. The TGA curve showed a weight loss in the range 50–158°C with a plateau up to 215°C corresponding to the loss of four water molecules. The plot of log σ vs. $1/T$ in Fig. 1(b) shows a peak (B) at about 85°C for the dehydration step [11]. The isothermally heated sample of $FeC_4H_4O_4 \cdot 4H_2O$ under static air at 160°C showed no H–OH bands in the IR spectrum, the XRD pattern showed

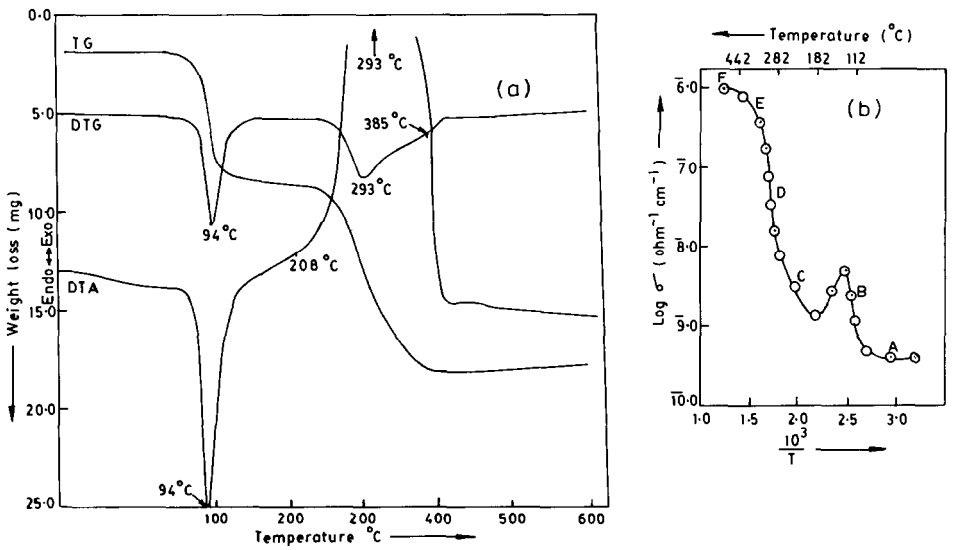

Fig. 1. Static air atmosphere. (a) TGA, DTA and DTG curves for $FeC_4H_4O_4 \cdot 4H_2O$. (b) Plot of log σ vs. $1/T$ for $FeC_4H_4O_4 \cdot 4H_2O$: (⊙) during decomposition.

TABLE 1

XRD data for an isothermally heated sample of $FeC_4H_4O_4 \cdot 4H_2O$ under dynamic nitrogen atmosphere

d-Spacings (Å)		
250°C	340°C	440°C
4.151 w	4.151 s	4.151 s
2.371 m	2.271 m	2.371 m
2.330 w	2.330 w	
2.304 w	2.304 w	
2.182 w	2.182 w	2.182 w
2.110 w	2.110 w	
2.052 s	2.052 s	2.052 s
1.945 w	1.945 w	1.945 w
1.465 w	1.465 w	

polycrystallinity of the sample with decrease in interplanar spacing (Table 1). The C and H analysis of this isothermally heated sample agreed well with the formula $FeC_4H_4O_4$ (anhydrous Ferrous succinate).

The oxidative decomposition step is represented by a strong and broad exothermic peak on the DTA curve at 293°C and by a strong peak at the same temperature on the DTG curve. A continuous weight loss was shown on the TGA curve in this region. Due to the broadness of the exothermic peak on the DTA curve and a continuous weight loss on the TGA curve, the various metastable intermediates formed during this step could not be detected by these curves. A complementary technique of measuring d.c. electrical conductivity, which is represented in Fig. 1(b) by a plot of log σ vs. $1/T$, showed different values of conductivities corresponding to the various intermediates formed during this oxidative decomposition step. After the dehydration step, the σ value steadily increased from 215 to 282°C (region C). The IR spectrum of the isothermally heated sample of $FeC_4H_4O_4 \cdot 4H_2O$ at 260°C showed a decrease in the intensities of the coordinated carboxylate bands; in addition bands at 290(s) cm^{-1} and 360(m) cm^{-1} occurred for metal–oxygen stretching frequencies due to the presence of iron oxide [12]. The XRD pattern of this isothermally heated sample was generally broad. Nevertheless peaks corresponding to both FeO and $FeC_4H_4O_4$ was observed.

Although a sharp increase in σ was observed at 285°C (region D) the characteristic high value of Fe_3O_4 (3.0 mho cm^{-1}) could not be obtained under dynamic conditions and a change in slope was observed at 350°C (region E), probably due to the formation of semiconducting γ-Fe_2O_3. The sample in region E (250–430°C) was mainly γ-Fe_2O_3 with traces of Fe_3O_4. The XRD pattern was generally broad showing peaks corresponding to γ-Fe_2O_3 and traces of Fe_3O_4. The IR spectrum of $FeC_4H_4O_4 \cdot 4H_2O$ heated

at 400°C, showed no bands corresponding to coordinated carboxylate bands, but strong, broad bands of Fe–O stretching frequencies were observed. Even the C and H analysis suggested no presence of any $FeC_4H_4O_4$. This part of the curve is followed by region F (i.e., above 445°C) corresponding to the complete reversible phase transformation of γ-Fe_2O_3 to α-Fe_2O_3.

When the reaction was carried out using the normal atmosphere, the gaseous products acted as a gas buffer for the solid state reaction and some of the reaction were ill defined. For example, the role of four water molecules in $FeC_4H_4O_4 \cdot 4H_2O$ and the role of atmospheric oxygen in the solid-state reaction carried out in the static air can be clarified by comparing the data of different physical properties for the reaction carried out in a dynamic (pure and dry) nitrogen atmosphere.

Dynamic nitrogen atmosphere

The dehydration step of $FeC_4H_4O_4 \cdot 4H_2O$ in Fig. 2(a) could be detected on the DTA curve by an endothermic peak at 121°C and a peak at the same temperature on the DTG curve. The TGA curve showed weight loss in the range 50–170°C corresponding to the loss of four water molecules. From 170 to 250°C the TGA curve shows a plateau indicating the stability of the anhydrous succinate ($FeC_4H_4O_4$) which is formed up to 250°C. A single strong peak (B) in the plot of log σ vs. $1/T$ in Fig. 2(b), corresponding to

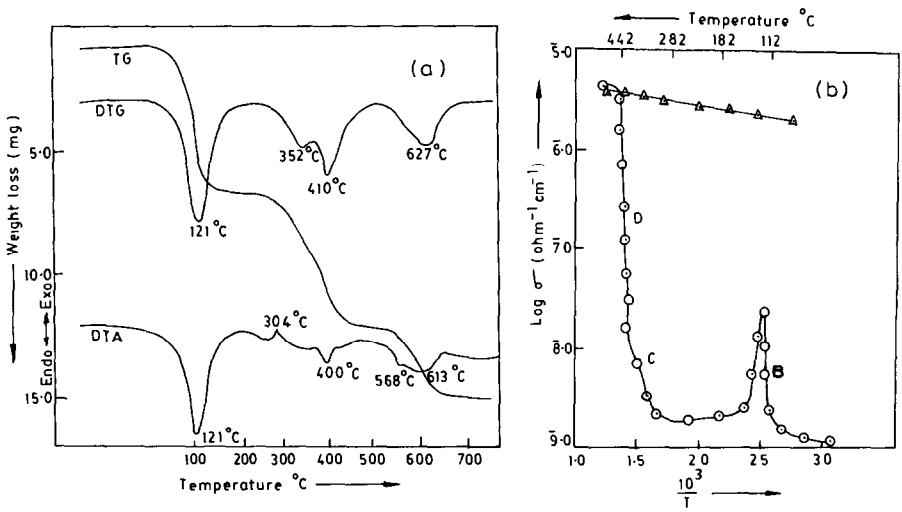

Fig. 2. Dynamic nitrogen atmosphere. (a) TGA, DTA and DTG curves for $FeC_4H_4O_4 \cdot 4H_2O$. (b) Plot of log σ vs. $1/T$ for $FeC_4H_4O_4 \cdot 4H_2O$: (⊙) during decomposition and (△) during cooling.

the dehydration step, was seen with further σ values remaining constant with temperature up to 250°C, thus verifying the stability of $FeC_4H_4O_4$. The stability was also confirmed by studying the IR spectrum and XRD pattern for the isothermally heated sample of $FeC_4H_4O_4 \cdot 4H_2O$ under this atmosphere at 250°C. The XRD pattern of this sample was generally crystalline (Table 1).

The endothermic peak of the DTA curve which corresponds to decomposition occurred at 400°C and that due to phase transformation to α-Fe_2O_3 at 613°C with a hump at 568°C. An exothermic peak at 304°C on the DTA curve may be due to the recrystallisation of the intermediate formed in that region. The peaks on the DTA curves are supported by peaks at similar temperature (i.e., 352, 410 and 629°C) on the DTA curve. After dehydration, the TGA curve showed two regions of weight loss, the first one from 253 to 518°C and the second from 530 to 680°C before its final crystallization to α-Fe_2O_3. However, the weight losses calculated from the TGA curve in these two regions did not reveal the formation of any particular single intermediate species. The plot of log σ vs. $1/T$ showed clearly the different intermediate phases which occurred during decomposition. Here the cooling curve was also noted to test the purity of the Fe_3O_4 formed. The sample obtained by isothermally heating $FeC_4H_4O_4 \cdot 4H_2O$ in region C (340°C) showed that the IR bands corresponding to Fe–O stretching frequencies became more intense, and that due to the coordinated carboxylate bonds decreased in intensity. The XRD pattern was very similar to that of the isothermally heated sample under static air at 260°C, indicating that the sample was a mixture of FeO and $FeC_4H_4O_4$; the difference seen in the

TABLE 2

XRD data of FeO and Fe_3O_4 obtained by isothermally decomposing $FeC_4H_4O \cdot 4H_2O$ under dynamic nitrogen atmosphere

FeO (cubic) *d*-spacings at 340°C (Å)	Fe_3O_4 (cubic) *d*-spacings at 440°C (Å)
	4.850 w
	2.967 m
	2.530 s
2.49 m	
	2.093 m
	1.609 m
1.523 s	
1.299 m	
	1.275 w
	1.091 w
1.077 w	
	0.967 w
	0.880 w
	0.812 w

TABLE 3

d-Spacings (Å) for FeO and Fe_3O_4

FeO (cubic) [20]	FeO (rhombohedron) [21]	Fe_3O_4 [22]
		4.850 (8) [a]
		2.967 (30)
		2.532 (100)
2.490 (80) [a]		2.424 (8)
2.153 (100)		2.099 (20)
		1.715 (10)
		1.616 (30)
1.523 (60)	1.525 (100) [a]	1.485 (40)
	1.512 (100)	1.419 (2)
		1.328 (4)
1.299 (25)	1.301 (20)	1.281 (10)
		1.266 (4)
	1.236 (60)	1.212 (2)
		1.122 (4)
		1.093 (12)
1.077 (15)	1.074 (60)	1.050 (6)
		0.9896 (2)
		0.9695 (6)
		0.9388 (4)
		0.8952 (2)
		0.8802 (6)
		0.8569 (8)
		0.8233 (4)
		0.8117 (6)
		0.8080 (4)

[a] Figures in parentheses show the relative line intensities, normalised to that of the strongest intensity line (given by 100).

XRD pattern under the nitrogen atmosphere was that the products obtained were more crystalline (Tables 1 and 2). The cooling curve of the sample at 440°C was not completely that of a metallic semiconductor type [6,12] it showed a decrease in σ value suggesting the presence of some other compound with Fe_3O_4. The sample of $FeC_4H_4O_4 \cdot 4H_2O$ when isothermally heated at 450°C under the same atmosphere, showed weakly coordinated carboxylate bands in the IR spectrum, the XRD pattern showed peaks corresponding mainly to Fe_3O_4 with some peaks corresponding to $FeC_4H_4O_4$ [13] (Tables 1 and 3). Thus on the basis of IR, XRD and elemental analysis it can be said that some $FeC_4H_4O_4$ was still present up to 450°C along with mainly Fe_3O_4, and it can be tentatively suggested that the presence of $FeC_4H_4O_4$ caused a decrease in the σ value during cooling [13,14].

Although the nature of decomposition and final products obtained from static air and dynamic (dry and pure) nitrogen atmospheres for $FeC_4H_4O_4 \cdot$

$4H_2O$ were similar, a few critical differences do exist. The main differences are:

(a) The TGA curve obtained under dynamic nitrogen atmosphere was resolvable and matched with the observed changes in log σ vs. $1/T$ plots, whereas the curve obtained under static air atmosphere was quite complex.

(b) The region E, corresponding to the γ-Fe_2O_3 formation stage, could not be identified under nitrogen atmosphere, whereas this region could be detected under static air atmosphere.

(c) The presence of some $FeC_4H_4O_4$ (anhydrous succinate) along with Fe_3O_4 was observed under dynamic nitrogen; this was not observed under static air atmosphere.

Since it is seen that the solid-state decompositions for $FeC_4H_4O_4 \cdot 4H_2O$ is highly influenced by the composition of the atmosphere, it would be advantageous to undertake similar measurements in other controlled atmospheres.

Dynamic air

The dehydration step was shown by an endothermic peak on the DTA curve at 101°C and a peak at the same temperature on a DTG curve. The TGA curve showed a weight loss from room temperature to 166°C, corresponding to the loss of four water molecules (Fig. 3a), a peak (B) was observed for this step in the plot of log σ vs. $1/T$ (see Fig. 3b). A strong exothermic peak for the oxidative decomposition step appeared at 326°C and a broad peak on the DTG curve at 330°C. The TGA curve showed continuous weight loss in this region until crystallisation to α-Fe_2O_3 occurred. These factors suggest that the formation of definite intermediates could not be shown by the thermal analysis curves under this atmosphere. However the plot of log σ vs. $1/T$ showed various regions of conductivities (viz. C, D and F).

The IR spectrum of the isothermally decomposed $FeC_4H_4O_4 \cdot 4H_2O$ sample showed a medium intensity band for the coordinated carboxylate group in region C, and strong bands due to Fe–O stretching frequencies. The XRD pattern of this sample was slightly broader having peaks corresponding to $FeC_4H_4O_4$ and FeO, the elemental analysis also indicated the presence of some $FeC_4H_4O_4$. Taking into consideration all these factors, it can be suggested that region C is a mixture of $FeC_4H_4O_4$ and FeO similar to region C under nitrogen and static air atmospheres. The study of region D on the basis of IR spectral data, elemental analysis and XRD pattern revealed that region D consists mainly of Fe_3O_4 with some $FeC_4H_4O_4$. The transformation of Fe_3O_4 into α-Fe_2O_3 is complete above 442°C, as indicated by region F.

A complete d.c. electrical conductivity study under the dynamic air containing water vapour was not possible as the pellet started melting above

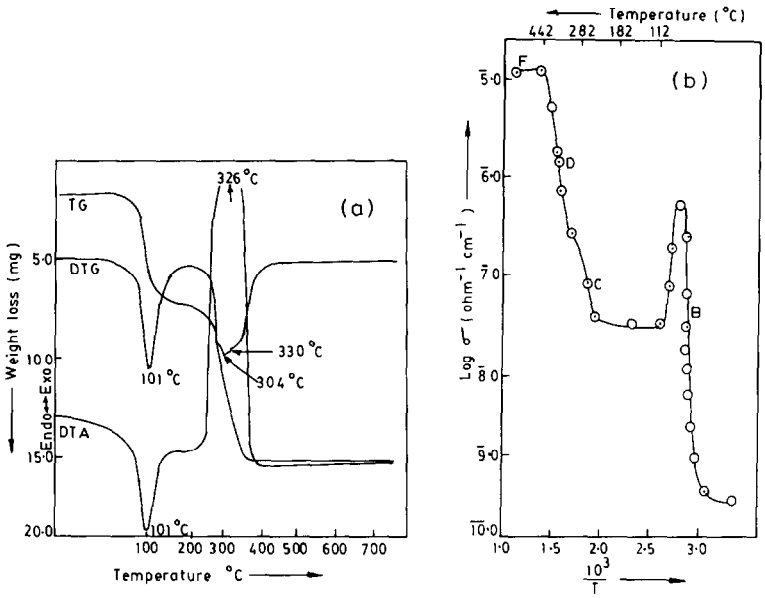

Fig. 3. Dynamic air atmosphere. (a) TGA, DTA and DTG curves for $FeC_4H_4O_4 \cdot 4H_2O$. (b) Plot of log σ vs. $1/T$ for $FeC_4H_4O_4 \cdot 4H_2O$: (⊙) during decomposition.

the dehydration temperature. However, formation of pure γ-Fe_2O_3 was possible by repeated trials of isothermally heating $FeC_4H_4O_4 \cdot 4H_2O$ under the same atmosphere at various ranges of temperatures [6,14,15]. From the trials it can best be suggested that pure γ-Fe_2O_3 could be obtained by isothermally heating $FeC_4H_4O_4 \cdot 4H_2O$ at 290°C for two and a half hours in a rotating flask furnace. The XRD pattern of γ-Fe_2O_3 thus obtained was tetragonal in configuration [16] (Table 4). The predicted intermediates obtained in each temperature region under all the atmospheres are given in Table 5.

The gases obtained by thermally decomposing $FeC_4H_4O_4 \cdot 4H_2O$ under dynamic (pure and dry) nitrogen atmosphere are represented by the chromatograms shown in Fig. 4(a, b). These chromatograms showed the presence of both types of gases, i.e., polar (viz. CO, CO_2, H_2, etc.) and non-polar gases (viz. CH_4, C_2H_6, C_3H_8, etc.). The gases were collected around 340°C.

The high-field HLT measurements at room temperature for γ-Fe_2O_3 in powder form, showed the H_C value to be 250 Oe, the M_S value to be 70 emu g^{-1} and the squareness ratio to be 0.55. All these values are in accordance with the room temperature theoretical values [3] for a single domain (SD) γ-Fe_2O_3 with the vacancy ordered configuration of $Fe_8^{3+}[Fe_{40/3}^{3+}\square_{8/3}]O_{32}$. Since γ-Fe_2O_3 is ferrimagnetic and α-Fe_2O_3 antiferromagnetic, initial susceptibility (X_i) measurements were employed to serve as a tool for determining the Curie temperature (T_C). On the basis of X_i and T measurements, the

TABLE 4

XRD data of γ-Fe_2O_3

d-Spacings (Å)				
Lattice planes (*hkl*)	γ-Fe_2O_3 (tetragonal) [23]		Observed [a]	
101	7.91	(1)		
102	6.94	(2)		
110	5.90	(6)		
112	5.33	(1)	5.33	(2)
113	4.82	(6)	4.82	(5)
114	4.29	(2)	4.28	(5)
210	3.73	(6)	3.73	(5)
213	3.40	(7)	3.39	(7)
214	3.20	(3)	3.21	(3)
220	2.95	(30)	2.95	(27)
300	2.78	(3)	2.79	(2)
310	2.64	(4)	2.64	(3)
313	2.51	(100)	2.51	(100)
226	2.41	(2)	2.398	(2)
320	2.32	(2)	2.33	(4)
323	2.23	(2)	2.23	(2)
400	2.09	(15)	2.08	(16)
420	1.87	(1)	1.86	(1)
423	1.82	(3)	1.82	(4)
426	1.70	(19)	1.69	(18)
430	1.67	(2)	1.67	(2)
513	1.604	(20)	1.59	(21)
520	1.55	(2)	1.55	(2)
523	1.53	(3)	1.52	(4)
440	1.47	(4)	1.47	(38)
620	1.32	(6)	1.31	(7)
539	1.27	(8)	1.27	(8)
626	1.26	(3)	1.26	(3)
442	1.20	(5)	1.92	(5)
646	1.12	(6)	1.11	(5)
733	1.09	(10)	1.08	(8)
800	1.043	(7)	1.04	(6)
826	0.98	(5)	0.98	(5)
753	0.96	(8)	0.96	(8)
840	0.93	(4)	0.93	(4)

[a] Observed *d*-spacing values of γ-Fe_2O_3 prepared from $FeC_4H_4O_4 \cdot 4H_2O$.

Curie temperature (T_C) for the γ-Fe_2O_3/α-Fe_2O_3 transformation is 792 K; furthermore, these measurements revealed the SD behaviour for the γ-Fe_2O_3 sample before its transformation into α-Fe_2O_3, with a well defined Hopkinson's peak [17].

The SEM of γ-Fe_2O_3 particles synthesised from $FeC_4H_4O_4 \cdot 4H_2O$, showed small spherical particles bound together to give particles of 1–6 μm

TABLE 5

Predicted intermediates and final product obtained from $FeC_4H_4O_4 \cdot 4H_2O$ under different atmospheres by d.c. electrical conductivity measurements

Atmosphere	Steps	Temperature range (°C)	Predicted intermediates and final product
Static air	B	85–184	$FeC_4H_4O_4$
	C	184–283	$FeC_4H_4O_4 + FeO$
	D	283–350	Fe_3O_4
	E	350–420	γ-Fe_2O_3
	F	> 420	α-Fe_2O_3
Dynamic nitrogen	B	60–290	$FeC_4H_4O_4$
	C	290–390	$FeC_4H_4O_4 + FeO$
	D	390–440	$FeC_4H_4O_4 + Fe_3O_4$
	E	> 440	α-Fe_2O_3
Dynamic air	B	47–110	$FeC_4H_4O_4$
	C	110–290	$FeC_4H_4O_4 + FeO$
	D	290–400	Fe_3O_4
	F	> 440	α-Fe_2O_3

in diameter (Fig. 5). The surface area of these particles is probably large and hence $FeC_4H_4O_4 \cdot 4H_2O$ may have possible application in heterogeneous catalysis [18].

The Mossbauer spectrum showed six well resolved narrow bands (half band width 0.285 mm) in the intensity ratio 3 : 2 : 1 : 1 : 2 : 3 and the value of the hyperfine field was found to be 493.8 ± 5.0 kOe, in agreement with the reported values [19].

CONCLUSIONS

This study showed the following important points on the solid-state decomposition of $FeC_4H_4O_4 \cdot 4H_2O$.

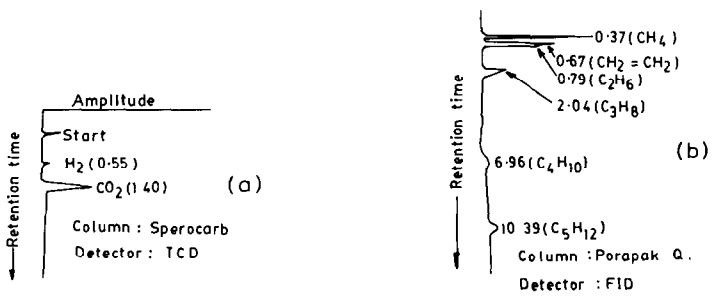

Fig. 4. Gas–liquid chromatograms for the gases obtained during the thermal decomposition of $FeC_4H_4O_4 \cdot 4H_2O$ under dynamic nitrogen atmosphere.

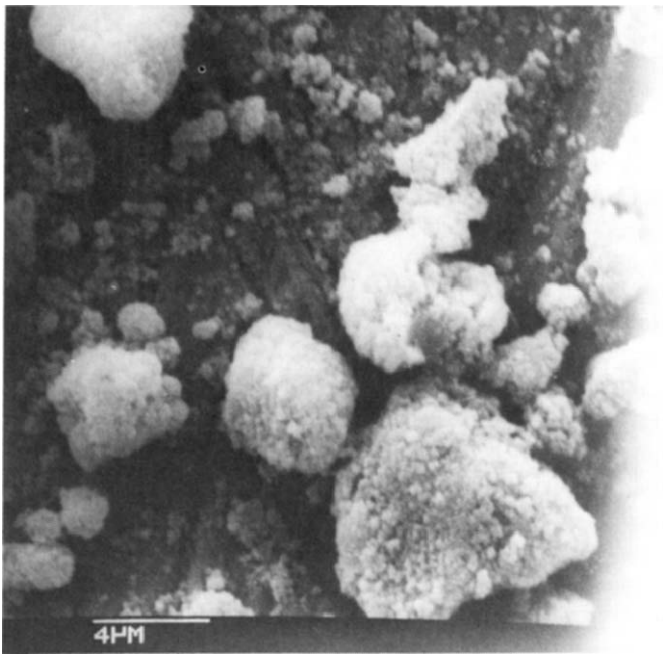

Fig. 5. SEM of γ-Fe_2O_3.

(a) The XRD pattern showed $FeC_4H_4O_4 \cdot 4H_2O$ and $FeC_4H_4O_4$ to be polycrystalline.

(b) The oxidative decomposition always followed dehydration under all the atmospheres.

(c) The conventional thermal analysis curves (TGA, DTA, DTG) showed a very broad and strong exothermic peak (DTA) and a continuous weight loss on TGA curves for the carboxylate under all the atmospheres at the oxidative decomposition step. These curves could not give information regarding the types of intermediates formed at this step. Hence it was found necessary to supplement these results with a more reliable technique, i.e., use of d.c. electrical conductivity measurements, IR spectral investigations and XRD methods.

(d) The final product of decomposition under all atmospheres is found to be α-Fe_2O_3.

(e) The gas chromatograms showed that both polar and non-polar gases were present during the thermal decomposition of $FeC_4H_4O_4 \cdot 4H_2O$.

(f) The high-field HLT and X_i and T measurements showed the required parameters of the γ-Fe_2O_3 synthesised sample to behave as an efficient magnetic tape recording material.

ACKNOWLEDGEMENT

The authors are grateful for the financial assistance given by Grants-in-aid (Ministry of Defence) Government of India.

REFERENCES

1 R.M. White, J. Appl. Phys., 57(1) (1985) 2996.
2 M.P. Sharrock and R.E. Bodnar, J. Appl. Phys., 57(1) (1985) 3919.
3 G. Bate, in D.J. Craik (Ed.), Magnetic Oxides, Vol. 2, Wiley-Interscience, London, 1975, Chap. 12.
4 R. Venkatesh, A.L. Sashimohan and A.B. Biswas, J. Mater. Sci., 9 (1974) 430.
5 K. Seshan, H.R. Anantharaman, R. Venkatesh, A.L. Shashimohan, H.V. Keer and D.K. Chakraborty, Bull. Mater. Sci., 3a (1981) 201.
6 K.S. Rane, A.K. Nikumbh and A.J. Mukhedkar, J. Mater. Sci., 16 (1981) 2387.
7 P.S. Bassi, B.S. Randhawa and H.S. Jamwal, Thermochim. Acta, 62 (1983) 209.
8 P.S Bassi, B.S. Randhawa and H.S. Jamwal, Thermochim. Acta, 65 (1983) 1.
9 H. YokoBayashi, K. Nagase and K. Muraishi, Bull. Chem. Soc. Jpn., 48(10) (1975) 2789.
10 W. Firc, Annalusius, 91 (1931) 30.
11 D.A. Deshpande, K.R. Ghormare, N.D. Deshpande and A.V. Tankhiwale, Thermochim. Acta, 62 (1983) 333.
12 A. Domenicale, Phys. Rev., 78(4) (1950) 458.
13 A. Venkataraman, A.K. Nikumbh, V.A. Mukhedkar and A.J. Mukhedkar, Proc. Indian Council of Chemists, University of Gorakhpur, 1984, pp. 10–15.
14 A. Venkataraman, V.A. Mukhedkar, A.K. Nikumbh and A.J. Mukhedkar, Proc. Ind. Acad. Sci., submitted.
15 A. Venkataraman, Ph.D. Thesis, University of Poona, Pune, India.
16 A.S.T.M. File no. 25-1402.
17 C.R.K. Murty, J. Geol. Survey Ind., 26 (1985) 640.
18 J.H. Sinfelt, in G.G. Libowitz and M.S. Whittingham (Eds.), Materials Science Series, Academic Press, New York, 1979, Chap. 1.
19 W.H. Kelly, V.J. Folen, M. Hass, W.N. Schreiner and G.B. Beard, Phys. Rev., 124 (1961) 80.
20 A.S.T.M. File No. 6-615.
21 A.S.T.M. File No. 6-711.
22 A.S.T.M. File No. 19-629.
23 E.W. Gorter, J. Phys. Radius, 12 (1951) 189.